IEEE Open Journal of
Industry Applications

Received 12 February 2023; revised 10 May 2023; accepted 13 May 2023. Date of publication 24 May 2023;
date of current version 7 June 2023. The review of this article was arranged by Associate Editor
Luca Solero.

Digital Object Identifier 10.1109/OJIA.2023.3279776

Single-Phase Mains Fed Three-Phase Induction Motor Drive Using Improved Power Quality Direct AC–AC Converter

TABISH NAZIR MIR [1], BHIM SINGH [2] (Fellow, IEEE), ABDUL HAMID BHAT [3], MARCO RIVERA [1] (Senior Member, IEEE), AND PATRICK WHEELER [1] (Fellow, IEEE)

[1]Department of Electrical and Electronic Engineering, University of Nottingham, NG7 2RD Nottingham, U.K.
[2]Department of Electrical Engineering, Indian Institute of Technology Delhi, New Delhi 110016, India
[3]Department of Electrical Engineering, National Institute of Technology Srinagar, Srinagar 190006, India

CORRESPONDING AUTHOR: TABISH NAZIR MIR (e-mail: mir.tabish.az@gmail.com)

This work was supported in part by ANID/ATE220023 Project; in part by FONDECYT Regular Research Project 1220556; in part by CLIMAT AMSUD 21001; and in part by FONDAP SERC Chile 15110019.

ABSTRACT This article presents an alternative ac–ac converter topology and its control for low-speed three-phase induction motor drives fed from single-phase ac mains. The proposed matrix converter based drive system eliminates the dc link capacitor, thus facilitating high power density and system reliability. The primary challenge in controlling a 1ϕ to 3ϕ matrix converter is to navigate the discrepancy of instantaneous power across the 1ϕ grid and 3ϕ load via a direct ac–ac converter. In order to address this concern, it is proposed to use mathematical modeling of the motor and input LC filter for state selection, in order to deliver improved current waveforms. Enhanced performance is demonstrated through simulations, and further validated using experimental results. Particularly improved power quality performance is achieved at low motor speeds, where precise low-speed sensorless operation is ensured through suitable speed observer.

INDEX TERMS AC–AC converter, 1ϕ to 3ϕ power converter, predictive control, motor drives, power quality, speed observer.

NOMENCLATURE

i_g, v_g	1ϕ grid current and voltage.
i_{in}, v_{in}	Current and voltage at converter input.
i_{abc}, v_{ab}	3ϕ motor currents and stator voltage (line-line).
ϕ_m, ϕ_r, ϕ_s	Magnetizing, rotor and stator magnetizing flux.
T_s	Sample time for predictions.
ω_b	Base frequency ($= 2\pi \times 50$) rad/s.
ω_r, ω_m	Electrical and mechanical rotor speeds.
θ_r	Rotor flux position.
R_s, R_r	Stator and rotor resistances.
X_{sl}, X_{rl}	Stator and rotor leakage reactances.
C_F, L_F, r_F	Input filter capacitance, inductance, and internal resistance of L_F.
I_r, I_s	Root mean square values of rotor and stator currents.
λ	Cost function weight for 1ϕ mains current.
x^{opt}	Predicted variable "x" for the most optimum switching state in the previous sample.
$\hat{x}$	Estimation of any variable "x.".
x^*	Reference value for any variable "x.".

I. INTRODUCTION

Electric motors are the most predominant loads on power networks worldwide, with three-phase (3ϕ) induction motors often being the most preferred choice due to their ruggedness, power density, and cost benefits. However, in a large number of consumer applications where 3ϕ power supply is not available, less efficient single-phase (1ϕ) motors are used. Alternatively, 3ϕ motors may be used on 1ϕ ac mains by using 1ϕ-3ϕ static power converters. Typically, multistage dc link converters are used to drive 3ϕ motors from 1ϕ ac sources [1]. Nonetheless, such converters often have a poor lifetime and increased footprint due to the use of dc link

TABLE 1. Comparison of 1ϕ-3ϕ Converter Topologies

	Unidirectional devices	Bi-directional devices	DC link/Decoupling capacitor	Boost inductance	Control Complexity
Proposed 1ϕ-3ϕ MC	0	6	0	0	Low
Back to Back VSCs	10	0	1	1	Low
Waghmare et al [6]	6	6	0	0	Moderate
Saito et al [7]	0	9	1	0	High

electrolytic capacitor. These capacitors are one of the leading causes of unreliability in motor drive systems [2]. Besides being a common point of failure, dc link capacitors hamper high power density. Especially in 1ϕ-3ϕ power converters, dc link capacitors are the most sizeable components in the drive due to the pulsating nature of 1ϕ power supplies. Although naturally commutated ac–ac converters have been previously proposed as a compact alternative [3], they exhibit significantly adverse power quality performance. Some topologies for 1ϕ-3ϕ static power converters are discussed in [4], [5], [6], [7], however, these have sizeable interdispersed energy storage elements and/or higher device count when compared to the topology considered here.

This article proposes the use of 1ϕ-3ϕ ac–ac matrix converter (MC) for driving a three-phase induction motor from a single-phase supply [8]. MCs are particularly popular for providing a nearly pure semiconductor solution for power conversion, which makes them much smaller than ac–dc–ac converter based drives [9]. Such motor drives are, therefore, ideal for applications where space and weight constraints exist. Additionally, in ac–dc–ac drives, the motor braking energy is fed back to the dc link capacitor, which needs to be sized enough to accommodate that energy, and be accompanied by a bleeder resistor to dissipate it. The MC-based drive besides being capacitorless is inherently bidirectional and feeds the braking energy from the motor back into the grid. Furthermore, in the coming years, monolithic bidirectional devices are expected to be commercialized and this could pave way for reducing the device count in MC fed drives. However, unlike 3ϕ-3ϕ MC, the converter is not quite popular in 1ϕ-3ϕ applications, due to an inevitable discrepancy in instantaneous power across this converter, which leads to distorted current waveforms on either the 3ϕ motor side [10] or the 1ϕ source side [11] of the converter. This article proposes a niche application and strategic control to overcome this limitation. A brief comparison of the proposed topology with previously documented converters for 1ϕ-3ϕ power conversion is outlined in Table 1.

The 1ϕ-3ϕ MC topology as shown in Fig. 1 has no significant energy storage devices. However, upon integration with a motor load and an input *LC* filter, distributed energy storage components are established in the circuit, which have potential to be strategically used to improve power quality metrics of the converter, especially with dedicated use in applications with low output frequency [8]. Thus, a low speed drive is an ideal candidate for such drives, so that the fluctuating 1ϕ ac power (pulsating at two times the frequency of 1ϕ ac mains), manifests itself as a high-order frequency corresponding to the low-frequency motor currents. Therefore, this fluctuating component can be smoothened out by the machine

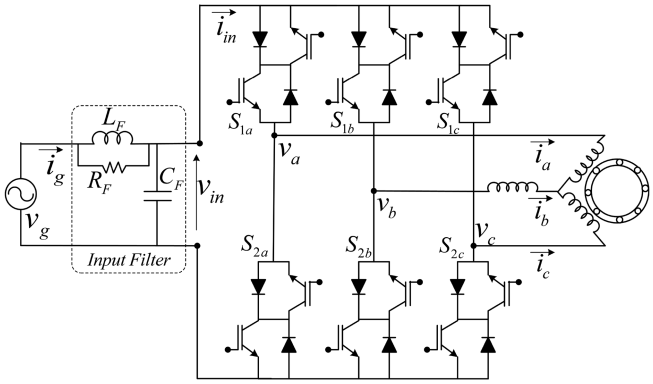

FIGURE 1. 1ϕ-3ϕ matrix converter fed induction motor drive.

inductances. In this article, speed sensorless control of a 1ϕ to 3ϕ matrix converter fed induction motor drive is presented for low speed applications. The MC is controlled using two objective model predictive control with finite control set [12], [13], which employs discrete models of the motor load and input *LC* filter, for concurrent control of 3ϕ motor currents and 1ϕ source current. Further, the article also proposes an improved motor speed observer for enhanced precision of the low speed estimate.

It is well known that flux estimation and encoderless performance over the low speed range are challenging due to factors such as converter voltage drops, integration offset, and parameter variation being significant at low stator frequency. For precise low speed estimates, various observers are reported in the available literature [14]. Among these, the full order Luenberger observer is a promising technique [15]. However, full order adaptive observers often exhibit stability issues at low speeds, particularly during regeneration as the motor traverses through zero speed. Available literature proposes a number of methods for overcoming stability problems near zero stator frequency. One of the widely accepted methods is based on gain scheduling for the observer gains [16] to achieve stable operation near zero frequency. This article uses the discretized model of the induction motor without any observer gains to predict the flux and stator current variables for each possible converter switch state. The challenge of precision in low speed estimation in the presence of 1ϕ grid power pulsation is tackled by means of refinements in the speed estimation algorithm. First, the rotor speed is determined from stator current errors in the synchronously rotating (dq) frame instead of the stationary frame of reference ($\alpha\beta$). This facilitates the use of digital filters to enhance the quality of estimated signals. An additional compensation term correlated with the error in d-component of motor current is used in generating a more precise rotor speed estimate.

The proposed drive system is a power-dense and reliable alternative for 3ϕ low-speed motor drives fed from 1ϕ ac mains in numerous consumer applications, such as automatic door closers, lifts and elevators, low speed centrifuges, treadmills, exercisers, conveyor belts, fuel filling machines at gas stations, and low-speed high volume fans.

The rest of this article is organized as follows. Two-objective finite set predictive control for 1ϕ-3ϕ matrix converter is described in Section II. The control of 3ϕ motor currents is detailed in Section II-A and that of 1ϕ ac mains current is outlined in Section II-B. Section III discusses state estimation and proposed modifications to attenuate 1ϕ power pulsations from the motor speed estimate. The proposed control and estimation algorithm is validated through simulation and experimental results reported in Section IV. Finally, conclusions regarding the suitability of 1ϕ-3ϕ MC fed drive are drawn in Section V.

II. TWO OBJECTIVE PREDICTIVE CONTROL FOR 1ϕ-3ϕ MATRIX CONVERTER

The main objective in 3ϕ-3ϕ matrix converter is often the concurrent control of grid currents and load voltages (or load currents). However, in the less explored 1ϕ-3ϕ MC topology, literature reports either sinusoidal 1ϕ source current or sinusoidal 3ϕ load waveforms [8]. Thus, one objective is achieved at the cost of compromise on the other control objective. This is because of the ineptitude of the ac–ac converter to handle instantaneous power imbalance between its two sides, in the absence of an intervening dc link [8]. Despite the fact, that lack of energy storage exacerbates power quality deterioration in this converter, it is crucial to retain this feature in order to impart compactness, high power density, and reliability in comparison to other ac–dc–ac converter counterparts.

This article addresses simultaneous power quality improvement on either side of the 1ϕ-3ϕ, in a targeted low output frequency application for 1ϕ mains fed motor drive systems. This is achieved by means of a two objective finite set model predictive control (TO-FS-MPC) technique, which mathematically models the grid side filter as well as the load side induction motor, for concurrent control on both sides of the converter. A sinusoidal source current with no reactive power flow inevitably generates an ac component in the source power, which pulsates at twice the grid frequency. To attenuate this 1ϕ pulsating component on the 3ϕ stator side, the drive is proposed for use in low speed applications. This implies that stator current harmonics that are produced due to pulsating component of 1ϕ power, present as harmonics of higher order in comparison to the fundamental stator currents at low frequency. Therefore, the algorithm uses the motor as an energy storage device to compensate for the lack of dc link energy storage, while the 1ϕ mains current quality is regulated by the input *LC* filter.

To undertake the control of 3ϕ motor currents, estimates of 3ϕ converter output voltages ($\hat{v}_{abc}^{j}$) for all converter states ($j = 0-7$) are needed. The input current estimate ($\hat{i}_{in}^{j}$) is required for 1ϕ mains current control. For this purpose, the converter switching possibilities, and representative estimates of 3ϕ output voltages and 1ϕ mains current are given in Table 2.

TABLE 2. Switched Variables in 1ϕ to 3ϕ AC–AC Converter

	Load Voltages			Mains Current
Switch State	$\hat{v}_{an}$	$\hat{v}_{bn}$	$\hat{v}_{cn}$	$\hat{i}_{in}$
000	0	0	0	0
001	$-\frac{1}{3}v_{in}$	$-\frac{1}{3}v_{in}$	$\frac{2}{3}v_{in}$	i_c
010	$-\frac{1}{3}v_{in}$	$\frac{2}{3}v_{in}$	$-\frac{1}{3}v_{in}$	i_b
011	$-\frac{2}{3}v_{in}$	$\frac{1}{3}v_{in}$	$\frac{1}{3}v_{in}$	$-i_a$
100	$\frac{2}{3}v_{in}$	$-\frac{1}{3}v_{in}$	$-\frac{1}{3}v_{in}$	i_a
101	$\frac{1}{3}v_{in}$	$-\frac{2}{3}v_{in}$	$\frac{1}{3}v_{in}$	$-i_b$
110	$\frac{1}{3}v_{in}$	$\frac{1}{3}v_{in}$	$-\frac{2}{3}v_{in}$	$-i_c$
111	0	0	0	0

A. CONTROL OF 3ϕ MOTOR CURRENTS

To control the motor currents, the commanded 3ϕ currents (i_{abc}^{*}) are generated through speed and flux controllers, using the standard vector control algorithm. The commanded dq components of motor currents in the synchronously rotating frame of reference are

$$i_q^* = \left(k_p^{\omega} + \frac{k_i^{\omega}}{s}\right)\left(\omega_m^* - \hat{\omega}_m\right)$$
$$i_d^* = \left(k_p^{\phi} + \frac{k_i^{\phi}}{s}\right)\left(\phi_r^* - \hat{\phi}_r\right). \tag{1}$$

Once the rotor flux position ($\hat{\theta}_r$) is determined, as discussed later in (11), the reference 3ϕ motor currents (i_{abc}^{*}) are further deduced from their dq components using inverse Park's transformations.

A discretized model of the induction motor is employed to compute flux as well as currents corresponding to each state of the 1ϕ-3ϕ MC. The discretized flux equations for the jth state are

$$\phi_{\beta s(n+1)}^{j} = T_s\omega_b\left[\hat{v}_{\beta}^{j} - \frac{R_s}{X_{sl}}\left(\phi_{\beta s(n)}^{opt} - \phi_{\beta m(n)}^{opt}\right)\right] + \phi_{\beta s(n)}^{opt}$$
$$\phi_{\alpha s(n+1)}^{j} = T_s\omega_b\left[\hat{v}_{\alpha}^{j} - \frac{R_s}{X_{sl}}\left(\phi_{\alpha s(n)}^{opt} - \phi_{\alpha m(n)}^{opt}\right)\right] + \phi_{\alpha s(n)}^{opt}$$
$$\phi_{\beta r(n+1)}^{j} = -T_s\omega_b\left[\frac{(-\hat{\omega}_r)}{\omega_b}\phi_{\alpha r(n)}^{opt} + \frac{R_r}{X_{rl}}\left(\phi_{\beta r(n)}^{opt} - \phi_{\beta m(n)}^{opt}\right)\right] + \phi_{\beta r(n)}^{opt}$$
$$\phi_{\alpha r(n+1)}^{j} = -\omega_b T_s\left[\frac{(\hat{\omega}_r)}{\omega_b}\phi_{\beta r(n)}^{opt} + \frac{R_r}{X_{rl}}\left(\phi_{\alpha r(k)}^{opt} - \phi_{\alpha m(n)}^{opt}\right)\right] + \phi_{\alpha r(n)}^{opt}$$
$$\phi_{\beta m(n+1)}^{j} = \frac{X_{eq}}{X_{sl}}\phi_{\beta s(n+1)}^{j} + \frac{X_{eq}}{X_{rl}}\phi_{\beta r(n+1)}^{j}$$

$$\phi^j_{\alpha m(n+1)} = \frac{X_{eq}}{X_{sl}}\phi^j_{\alpha s(n+1)} + \frac{X_{eq}}{X_{rl}}\phi^j_{\alpha r(n+1)} \tag{2}$$

where X_{eq} is defined as

$$X_{eq} = \frac{X_m X_{sl} X_{rl}}{X_m X_{sl} + X_{sl} X_{rl} + X_{rl} X_m}. \tag{3}$$

Then, predictions of motor currents are made from the flux variables given in (2)

$$\begin{aligned} i^j_{\beta s(n+1)} &= \frac{\phi^j_{\beta s(n+1)} - \phi^j_{\beta m(n+1)}}{X_{sl}} \\ i^j_{\alpha s(n+1)} &= \frac{\phi^j_{\alpha s(k+1)} - \phi^j_{\alpha m(n+1)}}{X_{sl}}. \end{aligned} \tag{4}$$

It must be noted that all reactance values are calculated with a base value of supply frequency, irrespective of the speed of the motor. As such these reactance values are constants, and immune to any changes in motor speed.

The 3ϕ current references are individually compared with predictions of motor currents for each converter state (i^j_{abc}). The resulting error ($e^j_{3\phi}$) constitutes the cost function that is eventually minimized

$$e^j_{3\phi} = \sum_{x=a,b,c} \left[i^*_{x(n+1)} - i^j_{x(n+1)} \right]^2. \tag{5}$$

B. CONTROL OF 1ϕ AC MAINS CURRENT

For the control of 1ϕ mains current, a suitable reference signal (i^*_g) needs to be generated. This article proposes to use the reference torque component $\left(\hat{\omega}_m \left(k^\omega_p + \frac{k^\omega_i}{s}\right)\left(\omega^*_m - \hat{\omega}_m\right)\right)$ to generate the source current reference (i^*_g). In fact, this implementation is an adapted version of active power balancing between both sides of the converter. Moreover, the motor copper losses are also incorporated in 1ϕ reference current generation. The amplitude of 1ϕ mains current command is therefore

$$i^*_g = \frac{\sqrt{2}}{V_g}\left[\hat{\omega}_m \left(k^\omega_p + \frac{k^\omega_i}{s}\right)\left(\omega^*_m - \hat{\omega}_m\right) + 3\hat{I}^2_s R_s + 3\hat{I}^2_r R_r\right]. \tag{6}$$

This adapted version of the input–output power balance offers better tracking performance, by continuing to adjust the source current reference until the motor attains the speed command, thereby overcoming any inadvertent performance deviation. Intuitively, $i^*_g(t)$ is allocated the same template as that of the 1ϕ mains voltage to warrant sinusoidal operation and IPF correction.

Ideally, 1ϕ mains current and 3ϕ load currents are sinusoidal signals. However, any attempted enhancement in 3ϕ motor current waveforms has detrimental effects on the 1ϕ mains current quality [11]. It is proposed to deal with this problem by modeling the input *LC* filter and the induction motor, and incorporating both models in the switching decision making process. The input filter model is given as

$$\begin{bmatrix} i^j_{g(n+1)} \\ v^j_{in(n+1)} \end{bmatrix} = \begin{bmatrix} 0 & (1-(r_F T_s/L_F)) \\ 1 & (T_s/C_F) \end{bmatrix} \begin{bmatrix} i^{opt}_{g(n)} \\ v^{opt}_{in(n)} \end{bmatrix} + \begin{bmatrix} \left(v_{g(n)} - v^j_{in(n)}\right) T_s/L_F \\ \left(-i^j_{in(n)} T_s/C_F\right) \end{bmatrix}. \tag{7}$$

The error between the reference 1ϕ current (i^*_g) and the predicted 1ϕ currents of all states, constitutes the other weighted objective of the cumulative cost function

$$e^j_{1\phi} = [i^*_{g(n+1)} - i^j_{g(n+1)}]^2. \tag{8}$$

TO-FS-MPC evaluates the cumulative cost function (F^j_{obj}) in each sample time, and makes the switching decision in favor of the least error state

$$F^j_{obj} = e^j_{3\phi} + \lambda e^j_{1\phi}. \tag{9}$$

As the switching state is found using TO-FS-MPS, predictions of flux variables (ϕ^{opt}), stator currents (i^{opt}_{abc}), 1ϕ grid current (i^{opt}_g), and voltage (v^{opt}_{in}) at input of the matrix converter for the least error state are carried forward. These optimum variables are recursively used in the control algorithm as feedback terms for the motor model, the filter model, and also for subsequent estimation of speed. Since the computation algorithm uses predictions of the winning state, it is possible to eliminate voltage sensor from input filter and current sensor from 1ϕ ac mains.

III. STATE ESTIMATION

To use vector control of the motor, it is essential to determine rotor flux ($\hat{\phi}_r$) and corresponding position ($\hat{\theta}_r$). Rotor speed measurement or estimation is also required. When a switch state is realized by TO-FS-MPC, rotor flux predictions of the best state are carried ahead to derive an estimate of the rotor flux

$$\hat{\phi}_r = \sqrt{\left(\phi^{opt}_{\beta r}/\omega_b\right)^2 + \left(\phi^{opt}_{\alpha r}/\omega_b\right)^2}. \tag{10}$$

Furthermore, the rotor flux position in electrical radians can be found

$$\hat{\theta}_r = \tan^{-1}\left(\phi^{opt}_{\beta r}/\phi^{opt}_{\alpha r}\right). \tag{11}$$

In line with (6), the generation of the 1ϕ grid current reference requires estimates of the 3ϕ stator current ($\hat{I}_s$), rotor current ($\hat{I}_r$), and rotor speed ($\hat{\omega}_m$). The stator current estimate corresponds to the prediction for the most optimum switching state

$$\hat{I}_s = \frac{1}{\sqrt{2}}\sqrt{\left(i^{opt}_{\beta s}\right)^2 + \left(i^{opt}_{\alpha s}\right)^2}. \tag{12}$$

Similarly, the rotor current estimate can be calculated from the optimum flux variables

$$i_{\beta r}^{opt} = \frac{\phi_{\beta r}^{opt} - \phi_{\beta m}^{opt}}{X_{rl}}, i_{\alpha r}^{opt} = \frac{\phi_{\alpha r}^{opt} - \phi_{\alpha m}^{opt}}{X_{rl}}$$
$$\hat{I}_r = \frac{1}{\sqrt{2}}\sqrt{\left(i_{\beta r}^{opt}\right)^2 + \left(i_{\alpha r}^{opt}\right)^2}. \quad (13)$$

Speed sensorless drive systems are well known to be more reliable and economically feasible as compared to measurement-based systems [14]. However, speed observation over the low speed range is challenging on account of parametric variation and significant resistive drops at low motor speeds. Generally, full order adaptive observers are most commonly preferred when a wide range of speed estimation is desired. Speed estimate in the synchronous reference frame for conventional full order estimators, is thereby given as

$$\hat{\omega}_m = -\left(k_p^{est} + \frac{k_i^{est}}{s}\right)\left(\frac{\phi_{dr}^{opt}}{\omega_b}(i_{qs} - i_{qs}^{opt})\right). \quad (14)$$

Considering the constraints of the converter and its proposed application, two modifications in the observer algorithm are made to enhance precision in speed estimation. These are,

1) As well as the quadrature axis stator current error, the speed update uses an additional compensation term with a factor (η) for the d-component of stator current error.
2) Digital low pass filtering is used for the dq-components of stator current errors. This enhances precision of the speed estimate by weakening the effects of 1ϕ grid power pulsations, as well as switching noise that may otherwise appear on the rotor speed estimate.

Hence, the modified speed estimate is

$$\hat{\omega}_m = \left(k_p^{est} + \frac{k_i^{est}}{s}\right)\left(\eta f(i_{ds} - i_{ds}^{opt}) - \frac{\phi_{dr}^{opt}}{\omega_b} f(i_{qs} - i_{qs}^{opt})\right) \quad (15)$$

where f denotes the low pass digital filter given by

$$f(y) = \left[\left(\frac{2}{1 + e^{-2y}}\right) - 1\right]. \quad (16)$$

Since motor drives are often susceptible to stator resistance drift, a stator resistance update algorithm is used to enhance the performance of the drive system during parametric inconsistency. This helps to overcome any variations or drift in stator resistance, thereby enhancing the speed estimation performance. The stator resistance can also be estimated using the filtered error terms described in (15)

$$R_s = R_s^0 + \left(\frac{k_R}{s}\right)\left(\eta f\left(i_{ds} - i_{ds}^{opt}\right) - \frac{\phi_{dr}^{opt}}{\omega_b} f(i_{qs} - i_{qs}^{opt})\right) \quad (17)$$

where R_s^0 is the initial assumption of stator resistance.

TABLE 3. System Specifications Used in Simulation/Experimental Analysis

3ϕ System Specifications	
1ϕ Grid Voltage	$50Hz$, $230V$
Input Filter Capacitor (C_F)	$5\ \mu F$
Input Filter Inductor (L_F)	$0.75\ mH$
Inductor Resistance (r_F)	$0.1\ \Omega$
Damper Resistor (R_F)	$70\ \Omega$
Step Time (T_s)	$5\ \mu s$ (Sim)/ $50\ \mu s$ (Exp)
3ϕ Induction Motor	
Nominal Power	$2.2kW$
Nominal Voltage	$230\ V\ (line)$
Pole Pairs	2
Nominal Speed	$150rad/sec$

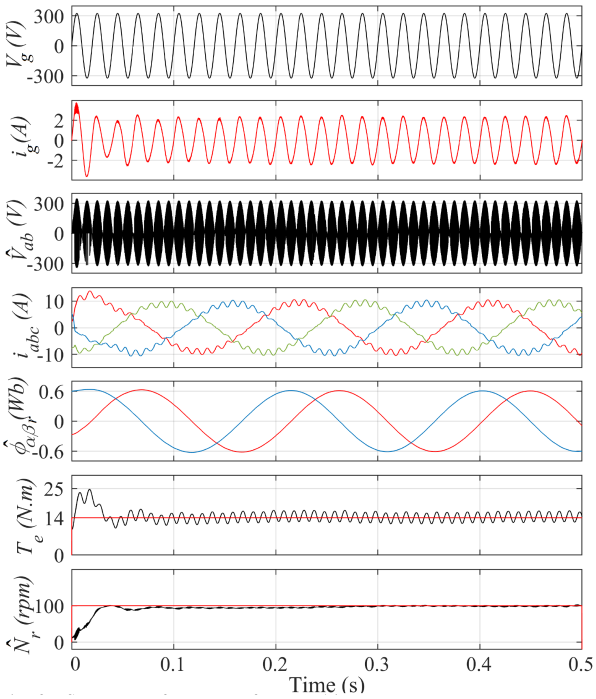

FIGURE 2. Start-up performance of motor drive.

IV. PERFORMANCE ANALYSIS

To validate the performance of the 1ϕ-3ϕ matrix converter fed motor drive, detailed simulation analysis and experimentation are undertaken. The proposed algorithm maintains a tradeoff between the 1ϕ source current and the 3ϕ stator current quality. The estimation technique is also validated. System parameters are given in Table 3. Simulations have been conducted using the same parameters of the filter and motor (Table 3) as used in experimentation. Experimentation has been carried out with a larger sampling time than the simulations, due to limitations of the controller dSPACE 1202 used in the tests. Test conditions, speed range, and load torque are similar for both validation environments.

A. SIMULATION RESULTS

The performance of the motor drive during low speed start up at rated torque, as shown in Fig. 2, which shows the 1ϕ ac voltage (v_g), 1ϕ mains current (i_g), the converter output voltage ($\hat{v}_{ab}$), the 3ϕ motor currents (i_{abc}), the stationary

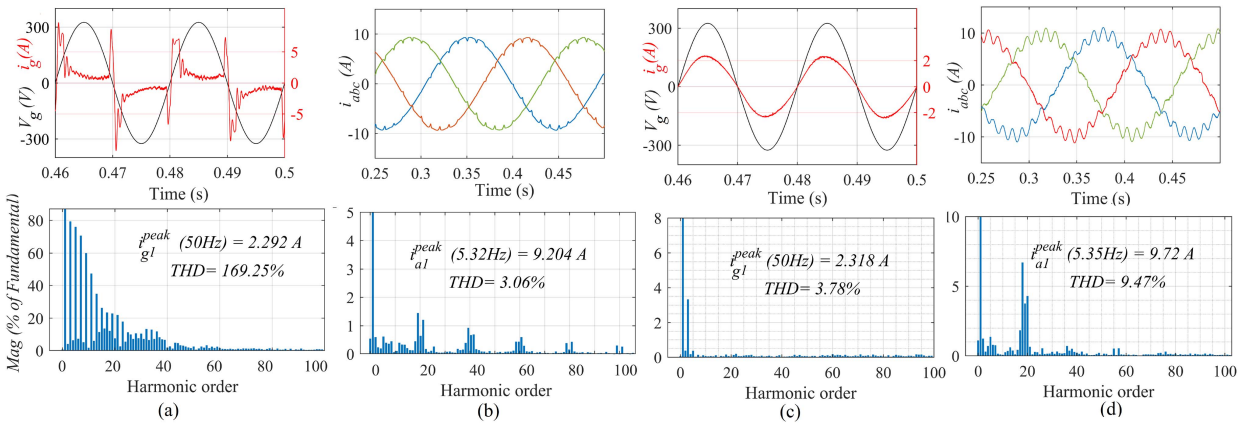

FIGURE 3. Comparative harmonic performance of 1ϕ-3ϕ MC fed motor drive with single and two-objective FS-MPC. (a) 1ϕ mains voltage and current with single-objective FS-MPC. (b) 3ϕ motor currents with single-objective FS-MPC. (c) 1ϕ mains voltage and current with two-objective FS-MPC. (d) 3ϕ motor currents with two-objective FS-MPC.

rotor flux signals ($\hat{\phi}_{\alpha\beta r}$), the electromagnetic torque (T_e), and the rotor speed estimate ($\hat{N}_r$). It can be seen that the source current waveform is sinusoidal and that the pulsating 1ϕ power is lower in the motor currents (at low stator frequency). Moreover, the flux variables ($\hat{\phi}_{\alpha\beta r}$) are completely sinusoidal, thus demonstrating the strategic use of motor load to compensate for the lack of energy storage in the converter.

Fig. 3 shows the comparative harmonic performance of single-objective FS-MPC for motor current control versus two-objective FS-MPC for the control of both grid and motor currents. Although, single-objective FS-MPC helps achieve optimum motor current waveforms [see Fig. 3(b)], the source current quality [see Fig. 3(a)] is poor with significant presence of lower order harmonics. It can be seen that grid current with TO-FS-MPC is sinusoidal with negligible reactive power flow, as observed in Fig. 3(c). It is a significant improvement over work reported in the past [11]. With sinusoidal mains current, the 1ϕ mains power pulsates at two times the grid frequency, which can have adverse impact on the load side due to lack of energy storage. It is possible to alleviate these fluctuations from appearing on the load side by modeling the distributed load and filter energy storage components, and subsequently incorporating these models into the control algorithm. The 3ϕ motor currents and corresponding harmonic profile for the proposed algorithm are shown in Fig. 3(d). The best balance of grid and motor current quality is achieved through two-objective FS-MPC.

The weighting factor is a critical parameter in multiobjective FS-MPC, as it determines the relative attainment of objectives. For cost functions involving more than a few weighting factors, optimal tuning of weighting factors is needed [17]. However, since this work is based on two-objective FS-MPC with only one weighting factor, i.e., λ for grid current control, this has been heuristically tuned for simplicity. Table 4 shows the choice of weighting factor λ and its effect on different power quality parameters such as total harmonic distortion (THD) in motor current, THD in grid current, distortion factor (DF), displacement factor (DPF), and input power factor (IPF).

TABLE 4. Effect of Weighting Factor on Power Quality Parameters

λ	% THD in i_{abc}	% THD in i_g	DF	DPF	IPF
0	3.06%	169.25%	0.5087	0.8729	0.4440
1	8.65%	20.46%	0.9797	0.9767	0.9569
5	9.16%	6.40%	0.9979	0.9983	0.9962
10	**9.47%**	**3.78%**	**0.9993**	**0.9995**	**0.9988**
12	9.81%	3.57%	0.9994	0.9997	0.9991
15	10.17%	3.02%	0.9995	0.9998	0.9993

An important aspect of the low speed drive is the estimation of motor speed. To show the efficacy of proposed revisions in the speed update law, the reference motor speed (N_r^*) and the estimated speed ($\hat{N}_r$) are given for different scenarios in Fig. 4. The classical speed estimator using traditional full order adaptive observer, that only uses q-component stator current error, is shown in Fig. 4(a). Fig. 4(b) shows the estimator performance with an additional factored (η) d-component of current error added in the speed update, besides the conventional q-component. Fig. 4(c) depicts the estimator performance with a digital low-pass filter (f) used over the q-component of error alone, and finally Fig. 4(d) shows the cumulative effect of digital low-pass filter (f) on both dq components of current errors. It is evident that the combination of both revisions in speed estimation law promises a more accurate speed estimate.

In Fig. 5, the performance of the stator resistance estimator (17) is shown for the drive during parametric inconsistency. Fig. 5(a) shows the speed estimation performance when the stator resistance is exactly known. Fig. 5(b) shows the speed estimation performance assuming a 15% error in stator resistance without any corrective estimator, and Fig. 5(c) shows the estimation performance with the online stator resistance estimator in place assuming a 15% error in stator resistance. The online stator resistance estimator takes necessary corrective action to rectify the value of stator resistance and eventually improves the speed estimation performance.

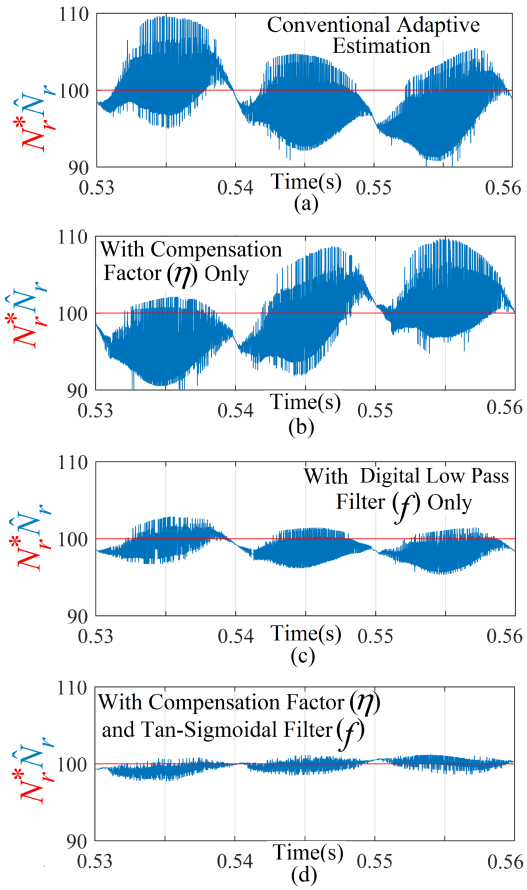

FIGURE 4. Estimation performance at low motor speed. (a) Classical adaptive estimation using just the *q* component stator current error. (b) Adaptive estimation with factored (η) *d* component stator current error. (c) Digital low-pass filter (*f*) used with classical adaptive estimator. (d) Performance with digital filter (*f*) on both *dq* stator current errors.

B. EXPERIMENTAL RESULTS

To validate the proposed control algorithm for the 1ϕ-3ϕ MC fed motor drive, a broad range of experimental results are presented. The steady-state performance of the drive is shown in Fig. 6. Fig. 6(a) shows the load voltage and 3ϕ load currents, Fig. 6(b) shows the $\alpha\beta$ plot of rotor flux, and Fig. 6(c) shows the steady-state reference and estimated rotor speed, and electromagnetic torque.

The steady-state grid side performance of the drive can be seen in Fig. 7. The 1ϕ grid voltage and grid current at unity input power factor are shown in Fig. 7(a), while the harmonic spectrum of source current is shown in Fig. 7(b), which has a total harmonic distortion (THD) of merely 3.3%. It must be noted that it is possible to further improve the quality of stator currents, by setting the weighting factor "λ" to zero in (9), however, this is achieved at the expense of severe lower order harmonics and poor THD in the grid current, which is undesirable.

The quality of the control and estimation algorithm is demonstrated through exhaustive speed control and torque perturbation in the low speed range, as shown in Fig. 8. The rotor speed is first decreased in steps of 50 r/min, and

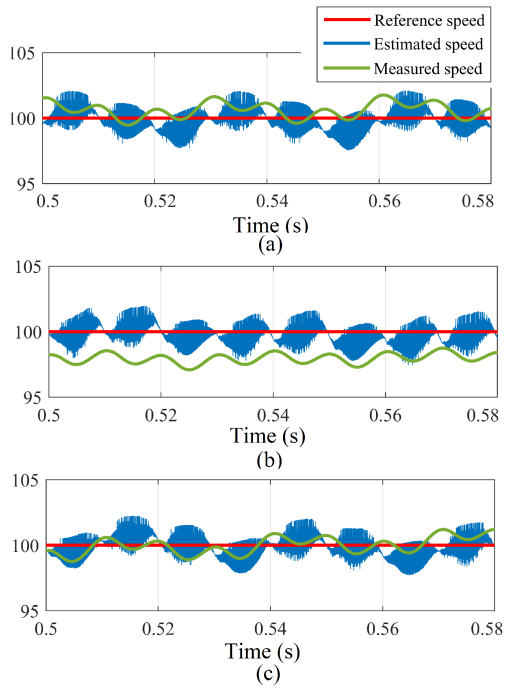

FIGURE 5. Reference, estimated and measured motor speeds. (a) Assuming that the stator resistance is exactly known (b) assuming a 15% error in stator resistance with no stator resistance estimator used (c) assuming a 15% error in stator resistance with a corrective online stator resistance estimator in place.

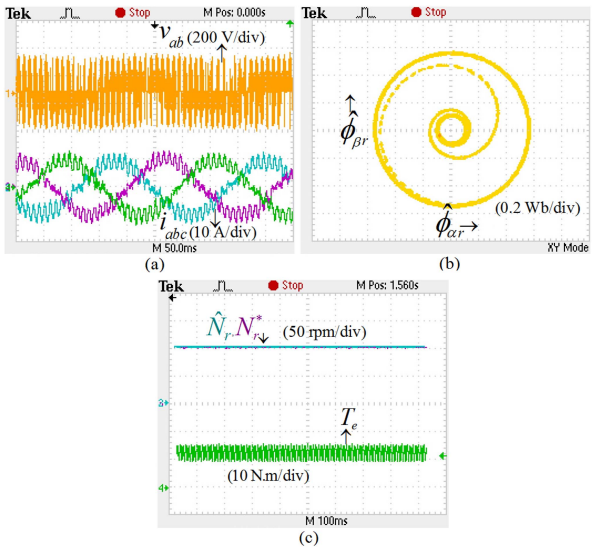

FIGURE 6. Experimental steadystate performance of 1ϕ-3ϕ MC fed drive. (a) Stator voltage and 3ϕ stator current. (b) $\alpha\beta$ plot of rotor flux. (c) Rotor speed and electromagnetic torque profile.

then further increased back to 100 r/min. The corresponding speed and torque dynamics are shown in Fig. 8(a). Fig. 8(b) shows the speed and torque dynamics as the motor is suddenly subjected to a torque perturbation from full load to no load.

Furthermore, the versatility of the motor drive is demonstrated by means of speed reversal. Fig. 9(a) shows

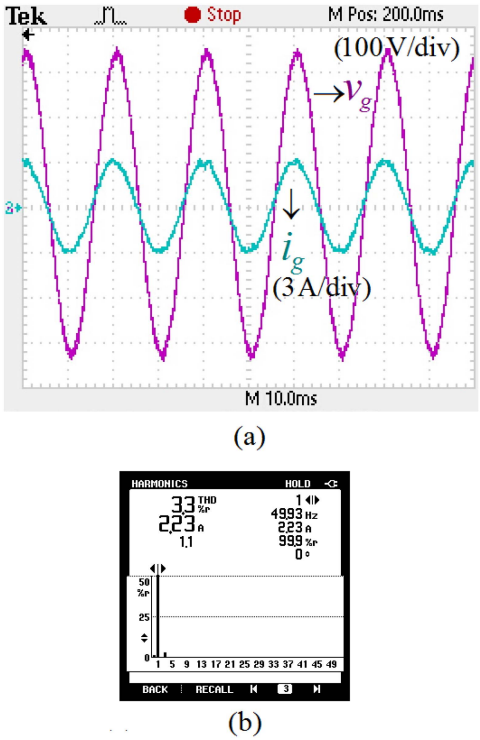

FIGURE 7. Experimental grid side performance. (a) 1ϕ grid voltage/current with no reactive power flow. (b) Harmonic analysis of grid current.

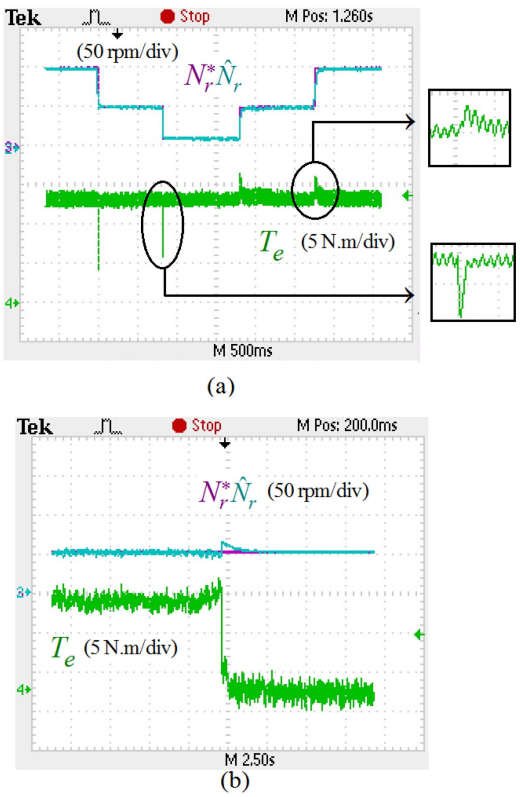

FIGURE 8. Experimental dynamic performance. (a) Speed control in the low speed region. (b) Sudden torque withdrawal.

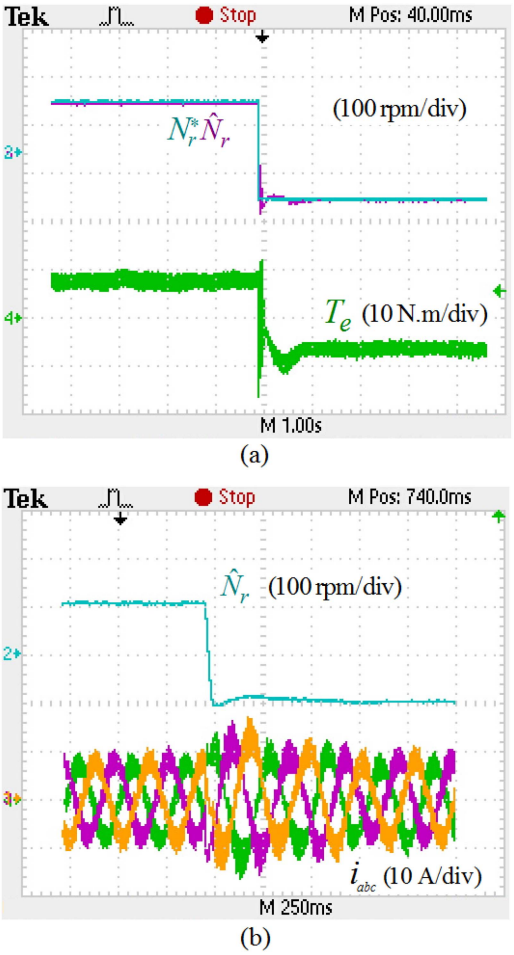

FIGURE 9. Experimental results for speed reversal (a) speed and torque reversal (b) speed and stator current phase reversal.

the dynamics in speed and torque as the command speed is reversed from +100 to −100 r/min, while corresponding reversal of phase in 3ϕ stator currents is shown in Fig. 9(b). It can be seen from Fig. 9(a) that the electromagnetic torque reverses once the rotor speed reverses. However, during the small interval when the motor is decelerating, the electromagnetic torque is still positive, and the motor operates under regenerative braking, feeding energy back to the grid.

V. CONCLUSION

In this article, it is concluded that high power density of 1ϕ-3ϕ MCs can be favorably exploited in consumer applications involving low-speed 3ϕ motor drives fed from 1ϕ ac mains. Through results and analysis it is demonstrated that despite the lack of dc energy storage, the mismatch in instantaneous power between the two sides of the converter can be mitigated, by accounting for the energy storage capabilities of the motor and input *LC* filter. This is achieved using mathematical models of the input filter and motor being incorporated in the switching decision process through TO-FS-MPC. The inherently low voltage conversion ratio of 1ϕ-3ϕ MC coupled with

the possibility of improved power quality at low stator frequency make this converter an ideal candidate for low speed drives. To achieve precision in low speed estimation, a full order predictive observer with revised speed update is presented. Digital low-pass filters are used on stator error terms to attenuate noise and power pulsations from the speed estimate. Additionally, the factored d component of stator current error can be employed while updating the speed estimate for increased overall precision. Impact of the revised speed update and efficacy of the control/switching algorithm in a low-speed motor drive are validated via simulation and experimental analysis. Thus, the 1ϕ-3ϕ MC fed low speed induction motor drive is advocated as a reliable and power-dense alternative, offering improved current quality for consumer applications like elevators, low speed centrifuges, automatic door closers, treadmills, exercisers, conveyor belts, fuel filling machines at gas stations, and low speed-high volume fans, operated from 1ϕ ac mains. Although limited by its operational range, this work can be further extrapolated to explore the suitability of 1ϕ-3ϕ MCs for low power-factor motors like synchronous reluctance machines and bespoke motor designs, where the performance metrics and speed range can be improved. The control concepts documented in this article can be used interchangeably for the control of single phase to three MCs in grid-tied applications with high-frequency ac link and grid frequency three phase output.

REFERENCES

[1] B. Kwak, J.-H. Um, and J.-K. Seok, "Direct active and reactive power control of three-phase inverter for AC motor drives with small DC-link capacitors fed by single-phase diode rectifier," *IEEE Trans. Ind. Appl.*, vol. 55, no. 4, pp. 3842–3850, Jul./Aug. 2019.

[2] M. Ghadrdan, S. Peyghami, H. Mokhtari, and F. Blaabjerg, "Condition monitoring of dc-link electrolytic capacitor in back-to-back converters based on dissipation factor," *IEEE Trans. Power Electron.*, vol. 37, no. 8, pp. 9733–9744, Aug. 2022.

[3] K. Smith and L. Ran, "Input current harmonic analysis of pseudo 12-pulse 3-phase to 6-phase cycloconverters," *IEEE Trans. Power Electron.*, vol. 11, no. 4, pp. 629–640, Jul. 1996.

[4] E. Cipriano, C. B. Jacobina, E. R. C. da Silva, and N. Rocha, "Single-phase to three-phase power converters: State of the art," *IEEE Trans. Power Electron.*, vol. 27, no. 5, pp. 2437–2452, May 2012.

[5] R. da Cruz Ferreira, S. M. A. Dias, N. Rocha, E. Ro. C. da Silva, and V. F. M. B. Melo, "Modulated predictive controller for a single-phase to three-phase converters with two parallel single-phase rectifiers," in *Proc. Braz. Power Electron. Conf.*, 2021, pp. 1–8.

[6] M. A. Waghmare, B. S. Umre, M. V. Aware, A. Iqbal, and A. Kumar, "Dual stage single-phase to multi-phase matrix converter for variable frequency applications," *IEEE Trans. Power Electron.*, vol. 38, no. 2, pp. 1372–1377, Feb. 2022.

[7] M. Saito and N. Matsui, "A single- to three-phase matrix converter for a vector-controlled induction motor," in *Proc. IEEE Ind. Appl. Soc. Annu. Meeting*, 2008, pp. 1–6.

[8] T. N. Mir, B. Singh, and A. H. Bhat, "Investigation on operational range and suitable control for single phase to three phase matrix converter," in *Proc. IEEE Energy Convers. Congr. Expo.*, 2021, pp. 2402–2407.

[9] H. Dan, P. Zeng, W. Xiong, M. Wen, M. Su, and M. Rivera, "Model predictive control-based direct torque control for matrix converter-fed induction motor with reduced torque ripple," *CES Trans. Elect. Mach. Syst.*, vol. 5, no. 2, pp. 90–99, 2021.

[10] P. Hothongkham, K. Poomphachana, and J. Songboonkaew, "Implementation of the single-phase AC-AC matrix converter without DC link," in *Proc. 18th Int. Conf. Elect. Eng./Electron., Comput., Telecommun. Inf. Technol.*, 2021, pp. 675–678.

[11] T. N. Mir, B. Singh, and A. H. Bhat, "Single-phase to three-phase matrix converter fed induction motor drive for low speed applications," in *Proc. IEEE Int. Conf. Power Electron., Drives Energy Syst.*, 2020, pp. 1–6.

[12] H. A. De Oliveira, B. C. Torrico, D. DeS. Oliveira, S. G. Barbosa, and M. P. De Almeida Filho, "Predictive control applied to a single-stage, single-phase bidirectional AC-DC converter," *IEEE Access*, vol. 10, pp. 34984–34995, 2022.

[13] T. N. Mir, B. Singh, and A. H. Bhat, "Single-phase to three-phase AC-AC converter FED low speed induction motor drive with encoderless control," in *Proc. IEEE Int. Conf. Power Electron., Smart Grid, Renewable Energy*, 2022, pp. 1–6.

[14] D. M. Stanica, N. Bizon, and M. C. Arva, "A brief review of sensorless ac motors control," in *Proc. 13th Int. Conf. Electron., Comput. Artif. Intell.*, 2021, pp. 1–7.

[15] L. Li, X. Huang, S. Zhang, and J. Wang, "Low-speed performance research of induction motor based on new speed adaptive method," in *Proc. IEEE 6th Adv. Inf. Technol., Electron. Autom. Control Conf.*, 2022, pp. 1633–1636.

[16] J. Yoo, I. Hwang, Y.-R. Lee, and S.-K. Sul, "Gain scheduling of full-order flux observer for sensorless pmsm drives considering magnetic spatial harmonics," in *Proc. IEEE Energy Convers. Congr. Expo.*, 2021, pp. 4769–4774.

[17] Y. Wei, D. Ke, H. Qi, and F. Wang, "A weighting factor semi-online tuning method based on correlation look-up table for model predictive torque control on PMSM of EV," in *Proc. IEEE 5th Int. Elect. Energy Conf.*, 2022, pp. 2138–2144.

TABISH NAZIR MIR received the B.Tech. degree in electrical engineering from National Institute of Technology, Srinagar, India, in 2014. She received the Ph.D. degree in power electronics and electric drives from the Indian Institute of Technology (IIT) Delhi, New Delhi, India, in 2020.

From 2020 to 2021, she was an Assistant Professor with the National Institute of Technology Srinagar, India. From 2021 to 2022, she was a Research Fellow with the Birmingham Centre for Railway Research and Education, University of Birmingham, where she is now an Honorary Research fellow. Thereafter, she joined as Research Associate at the Dyson Future Power Systems Lab, Newcastle University, where she worked on high-frequency power electronics for motor drive applications. In March 2023, she joined the Power Electronics and Machines Control (PEMC) Research Group, University of Nottingham as an Assistant Professor. Her research interests include design, modulation, and control of power converters, matrix converter fed motor drives, sensorless control of ac motors, wide band gap power converters, power electronics in railway applications, and power quality.

BHIM SINGH (Fellow, IEEE) received the B.E. degree in electrical engineering from the University of Roorkee, Roorkee, India, in 1977 and the M.Tech. degree in power apparatus and systems and the Ph.D. degree in electrical engineering from IIT Delhi, New Delhi, India, in 1979 and 1983, respectively.

In 1983, he joined the Department of Electrical Engineering, University of Roorkee, as a Lecturer. He became a Reader there in 1988. In December 1990, he joined the Department of Electrical Engineering, IIT Delhi, India, as an Assistant Professor, where he has become an Associate Professor in 1994 and a Professor in 1997. He has been ABB Chair Professor from 2007 to 2012. He has been the Head of the Department of Electrical Engineering, IIT Delhi from July 2014 to August 2016. He has been the Dean, Academics at IIT Delhi from August 2016 to August 2019. He has been JC Bose Fellow of DST from December 2015 to June 2021. He is the SERB National Science Chair Professor at IIT Delhi since July 2021. He has guided 114 Ph.D. dissertations, and 176 M.E./M.Tech./M.S.(R) theses. He has filed 105 patents. He has executed 90 sponsored and consultancy projects. He has coauthored a textbook on power quality: Power Quality Problems and Mitigation Techniques published by John Wiley & Sons Ltd. 2015. His areas of interest include solar PV grid interface systems, microgrids, power quality mitigation, solar PV water pumping, improved power quality ac–dc converters and electric vehicles.

ABDUL HAMID BHAT was born in Srinagar, India. He received the B.Tech. degree in electrical engineering from the National Institute of Technology (NIT) Srinagar (Then REC), Srinagar, India, in 1992, the M.Tech. degree in power electronics, machines, and drives and the Ph.D. degree in power electronics from Indian Institute of Technology Roorkee, Roorkee, India, in 2001 and 2007, respectively.

He is currently a Professor with the Department of Electrical Engineering, NIT Srinagar. His research interests include power electronics, electrical drives, high power converters, matrix converters, FACTS, and power quality.

MARCO RIVERA (Senior Member, IEEE) received the electronic civil engineering degree and the M.Sc. degree in engineering with specialization in electrical engineering from the Universidad de Concepción. He received the Ph.D. degree in electronic engineering from the Universidad Técnica Federico Santa María, and was awarded with the "Premio Tesis de Doctorado Academia Chilena de Ciencias 2012," for the best Ph.D. Thesis developed in 2011 for national and foreign students in any exact or natural sciences program, that is member of the Academia Chilena de Ciencias, Chile.

PATRICK WHEELER (Fellow, IEEE) received the B.Eng. (Hons.) degree from the University of Bristol, U.K., in 1990. He received the Ph.D. degree in electrical engineering for his work on matrix converters from the University of Bristol, Bristol, U.K., in 1994.

In 1993, he moved to the University of Nottingham and worked as a Research Assistant with the Department of Electrical and Electronic Engineering. In 1996, he became a Lecturer in the Power Electronics, Machines and Control Group, University of Nottingham, U.K. Since January 2008, he has been a Full Professor in the same research group. He is currently the Global Engagement Director for the Faculty of Engineering, the Head of the Power Electronics, Machines and Control Research Group, and the Director of the University of Nottingham's Institute of Aerosapce Technology. He was the Head of the Department of Electrical and Electronic Engineering, University of Nottingham from 2015 to 2018. He is a member of the IEEE PELs AdCom and is currently IEEE PELS Vice-President for Technical Operations. He has published more than 850 academic publications in leading international conferences and journals.